

1 **Rapid and accurate quantification of viable *Listeria monocytogenes* with clonal**
2 **specificity using microfluidic droplet digital PCR based technology**

3 Chi Song^{1, 2 #}, Zehang Gao^{3 #}, Gaoze Cai^{3, 4, 5}, Yongjie Yu⁶, Ruihua Ding^{2*}, Shilun Feng³,
4 Yangtai Liu^{1*}

5 ¹ University of Shanghai for Science and Technology, 200098, Shanghai, China

6 ² Shanghai Industrial μ Technology Research Institute (SITRI), 201800, Shanghai, China

7 ³ Key Laboratory of Transducer Technology, Shanghai Institute of Microsystem and
8 Information Technology, Chinese Academy of Sciences, Shanghai 200050, China

9 ⁴ Shanghai Frontier Innovation Research Institute, Shanghai 201108, China

10 ⁵ Xiangfu Laboratory, Jiashan 314100, China

11 ⁶ School of Materials Engineering, Changzhou Vocational Institute of Industry Technology,
12 Changzhou 213164, China

13

14 # These-authors contributed equally to this work.

15 *Corresponding authors

16

17 **Abstract**

18 To overcome the technical bottlenecks in the precise quantification and molecular typing of
19 viable foodborne pathogens, this study establishes a microfluidic droplet digital PCR (ddPCR)
20 based method for rapid and accurate detection and quantification of viable *Listeria*
21 *monocytogenes* with clonal specificity. In contrast to the time-consuming plate culture
22 methods and unspecific rapid detection methods, the method in this study employs clonal
23 complex (CC) specific primers and probe for strain-specificity and integrate the nucleic acid
24 dye propidium monoazide (PMA) to effectively distinguish viable from dead bacteria. The
25 rapid and precise quantification of viable bacteria is achieved through microdroplet counting.
26 This method does not require DNA extraction, and the entire detection process takes only
27 about 3 hours, with a quantitative detection limit of 3.3×10^2 CFU/mL, providing strong
28 technical support for the risk monitoring of highly pathogenic specific types of *L.*
29 *monocytogenes*.

30 Keywords: *L. monocytogenes*, clonal complex, microfluidic, ddPCR, PMA, quantitative
31 detection

32

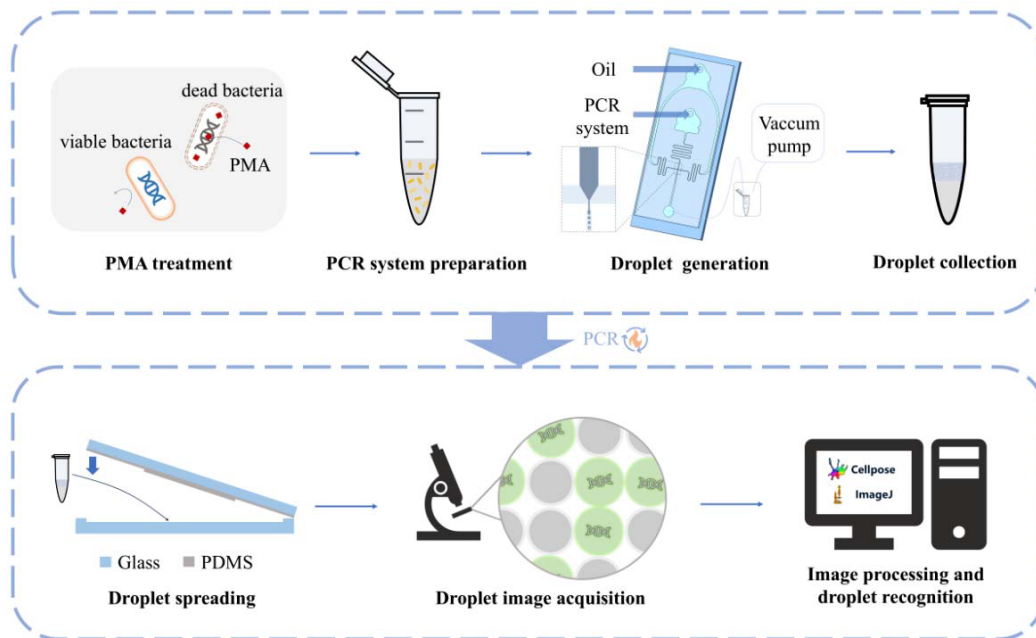
33 **1. Introduction**

34 Food safety is a critical issue concerning global public health and socio-economic
35 development. One of the primary food safety hazards is foodborne disease caused by
36 foodborne microorganisms [1]. These diseases severely threaten public health and hinder
37 global economic development [2–5]. The World Health Organization estimates that
38 approximately 600 million cases of foodborne illnesses occur worldwide each year, resulting
39 in 420,000 deaths. Additionally, low- and middle-income countries suffer annual losses of
40 \$110 billion in productivity and medical expenses due to unsafe food [6]. *Listeria*
41 *monocytogenes* is a facultative anaerobic foodborne pathogen that is widely present in the
42 environment and food. It can survive under low temperatures, acidic environments, high salt
43 concentrations, and other harsh conditions, often contaminating dairy products, vegetables,
44 fish, meat products, and ready-to-eat foods [7]. Over 99% of human listeriosis cases are
45 foodborne. High-risk groups susceptible to listeriosis include pregnant women, newborns,
46 cancer patients, the elderly, and immunocompromised individuals, with a fatality rate as high
47 as 20 ~ 30% [8,9]. The European Food Safety Authority (EFSA) reported 2,952 confirmed
48 cases of listeriosis caused by *L. monocytogenes* in Europe in 2023 [10]. According to the U.S.
49 Centers for Disease Control and Prevention, *L. monocytogenes* causes approximately 1,600
50 cases of foodborne illness and 260 deaths annually [11]. In China, a total of 562 sporadic
51 cases were reported from 2011 to 2017 [12]. Therefore, *L. monocytogenes* pose a threat to
52 global food safety and human health [13].

53 Currently, the internationally recognized gold standard for detecting viable *L. monocytogenes*
54 in food is the culture-based plate counting method. However, the cultivation process is
55 time-consuming, involves cumbersome operations, demands strict environmental and
56 operational conditions, and potentially leads to the oversight of viable but nonculturable
57 (VBNC) cells [14–16]. Although the automated systems for colony inoculation and counting
58 methods [17,18] can significantly enhance operational efficiency, the substantial time required
59 for bacterial isolation and cultivation remains unresolved. This significant time lag severely
60 restricts the timely response capabilities of food safety regulation and industrial quality
61 control. To overcome the drawback of the delayed results from culture-based counting
62 methods, several rapid detection techniques have been developed and applied. Rapid
63 detection methods often utilize dyes to achieve quick differentiation and quantification of
64 viable and dead bacteria. For instance, flow cytometry is frequently combined with dyes such
65 as SYTO9/PI [19] and TO/PI [20]. Meanwhile, methods based on Calcein AM [21] or
66 tetrazolium salt reduction and color development, such as MTT [22] and WST-8 [23], as well
67 as ATP bioluminescence methods based on luciferin and luciferase [24], have been developed
68 and typically the fluorescence intensity or absorbance are measured using a hand-held

69 fluorometer or a microplate reader. These methods then establish a standard curve accordingly
70 to quantify bacterial concentration. The rapid detection techniques are faster and more
71 convenient than traditional culture methods and enable high-throughput data acquisition.
72 However, for the specific detection of bacterial species, viable and dead stains cannot achieve
73 the clonal complexes (CCs) typing of strains, which is crucial for tracing infection sources,
74 identifying dominant pathogenic lineages, and studying the epidemiological characteristics of
75 strains. Therefore, we urgently need a detection method that integrates speed, high accuracy,
76 the ability to distinguish CCs typing, and precise quantification of viable bacteria.

77 Here we develop a microfluidic droplet digital PCR (ddPCR)-based method to rapidly and
78 accurately quantify bacteria with viable/dead distinguishing and CC typing (Fig. 1.). To
79 demonstrate CC typing, we detect the most frequently detected typing in clinical *L.*
80 *monocytogenes* isolates in China—clonal complex 87 (CC87) [25–27]. By integrating
81 propidium monoazide (PMA) pretreatment with droplet image processing and counting
82 analysis, this method innovatively achieves rapid identification and quantification of viable
83 CC87 *L. monocytogenes*. This method achieves a quantification limit of 3.3×10^2 CFU/mL and
84 completes the entire process within 3 hours, demonstrating high sensitivity and speed. When
85 applied in samples with mixed strains and mixed species, this method successfully achieves
86 strain-specific differentiation and precise quantification of viable bacteria. Overall, this
87 technology effectively overcomes the aforementioned technical bottlenecks, achieves rapid
88 and accurate detection of viable bacteria with CC typing, and provides a reliable tool for risk
89 monitoring of highly pathogenic subtypes.



91 Fig. 1. Procedure for rapid quantitative detection of viable *Listeria monocytogenes* clonal
92 complex 87 based on microfluidic droplet digital PCR.

93

94 **2. Materials and methods**

95 **2.1 Bacterial sample preparation and DNA extraction**

96 Two strains of CC87 *L. monocytogenes*, MRL 300112 and MRL 300131, isolated in our
97 laboratory, are selected as the test subjects. Frozen stocks of bacteria are maintained in
98 Tryptone Soy Yeast Extract Broth (TSB-YE; Qingdao Haibo Biotechnology Co., Ltd.,
99 Qingdao, China) with 50% glycerol at -80°C. Working stocks are stored at 4°C on Tryptone
100 Soy Agar with 0.6% Yeast Extract (TSA-YE; Qingdao Haibo Biotechnology Co., Ltd.,
101 Qingdao, China) and are renewed monthly. Prior to each experiment, a single colony is
102 inoculated into 10 mL of TSB-YE and incubated in a shaker at 180 rpm and 37°C for 16 ~ 18
103 h until reaching the stationary phase, resulting in an initial bacterial suspension with a
104 concentration of approximately 10⁹ CFU/mL, which serves as the working solution.
105 Preparation of dead bacterial suspension: Take the aforementioned working solution and treat
106 it at 100°C for 15 min to obtain dead bacterial cells of *L. monocytogenes*. The viability of the
107 cells can be confirmed by spreading them on TSA-YE and incubating at 37°C for 24 h; the
108 absence of colony growth indicates dead bacterial cells. DNA extraction is performed using a
109 DNA extraction kit (Tiangen Biotech, Beijing, China).

110 **2.2 Target DNA fragment, primers and probe**

111 Based on the SNP comparison analysis of 348 different CC-type *L. monocytogenes* strains,
112 including 12 CC87 *L. monocytogenes* as shown in Fig. S1 Specific sequence fragments of
113 CC87 *L. monocytogenes* are selected based on SNP comparison for the design of primers and
114 probe. These primers and probe are subjected to homology comparison analysis on the
115 BLAST platform of NCBI to verify their specificity. After confirmation, the synthesis is
116 commissioned to Sangon Biotech (Shanghai, China) Co., Ltd.

117 **2.3 Optimization of PCR reaction conditions**

118 The amplification procedure and system are optimized through qPCR. The combination
119 showing the lowest Ct value and the highest Rn value in qPCR results is considered optimal,
120 which could enhance the amplification efficiency in subsequent ddPCR and increases the
121 fluorescence intensity of positive droplets, thereby facilitating the distinction between positive
122 and negative droplets. The qPCR reaction system was 20 µL, comprising qPCR premix
123 (Sangon Biotech, Shanghai, China), 10 µM primers, 10 µM probe, ddH₂O, and template
124 DNA. The qPCR amplification procedure was as follows: 94°C for 10 min; 40 cycles of 94°C
125 for 5s and 60°C for 30s, with fluorescence signal collection. Using CC87 *L. monocytogenes*

126 (MRL 300112) as the positive template, the annealing temperature was optimized, and the
127 usage amounts of primers and probe were screened. The procedure is tested at eight different
128 annealing temperatures: 50°C, 52°C, 54°C, 56°C, 58°C, and 60°C, using the recommended
129 primers/probe concentration of 200/100 nM. At the optimal annealing temperature, the final
130 concentration ratios of primers/probe are set at 200/300 nM, 200/250 nM, 200/200 nM,
131 200/150 nM, 200/100 nM, and 200/50 nM.

132 **2.4 Optimization of PMA treatment**

133 Dissolve 1 mg of PMA (Aladdin, Shanghai, China) in 980 μ L of distilled water to obtain a 2
134 mM stock solution, which is then set aside. Accurately measure a certain volume of the 2 mM
135 PMA and add it to the sample to achieve a specific final concentration of PMA in the
136 PMA-sample mixture. Thoroughly mix the sample and incubate it in a dark room for 15
137 minutes to allow PMA to penetrate dead cells and attach to DNA, ensuring full penetration of
138 PMA into both dead and viable cells. After the dark treatment, place the sample in the
139 PMA-Lite™ LED Photolysis Device (Biotium) and expose it to LED light (460 nm) for 15
140 minutes to induce the device of PMA with DNA from dead cells. After crosslinking,
141 centrifuge the PMA-sample mixture at 10,000 rpm for 1 min, wash it twice with PBS
142 (Adamas, Shanghai, China) to collect bacterial cells, and subsequently use it for DNA
143 extraction and PCR. Dead and viable bacterial suspensions of *L. monocytogenes* are mixed
144 with different volumes (0, 2.5, 5, 7.5, 10, 12.5, 15, 17.5, and 20 μ L) of PMA solution to
145 obtain PMA-sample mixtures with varying final PMA concentrations (0, 10, 20, 30, 40, 50,
146 60, 70, and 80 μ M). These PMA-sample mixtures are pre-treated as described above,
147 followed by bacterial DNA extraction using the aforementioned method, and finally subjected
148 to quantitative fluorescent PCR analysis. Observe the test results to analyze and obtain the
149 optimal PMA treatment conditions.

150 **2.5 Design and fabrication of the microfluidic chip**

151 Design the pattern of the droplet generation chip using AutoCAD 2019. Use SU-8 3025 as the
152 photoresist and a silicon wafer as the substrate to fabricate the mold through MicroWriter
153 ML3 maskless lithograph (Durham Magneto Optics, UK). Development is completed by
154 immersion in 1-methoxy-2-propyl acetate (Sigma-Aldrich). After manufacturing the silicon
155 wafer mold, the next step is to create the microfluidic chip using polydimethylsiloxane
156 (PDMS, Sylgard184, Dow Coming, USA). Mix the PDMS base and curing agent in a 10:1
157 ratio, stir evenly, and then place it in a vacuum chamber to remove bubbles. Pour the mixture
158 onto the silicon wafer wrapped in tin foil and place it on a hot plate at 90°C for 2 hours. Use
159 tweezers to peel the obtained PDMS from the mold, cut it to the appropriate size, and use a
160 puncher to create holes at the reserved locations on the chip. Place the cleaned glass slide,
161 which has been washed with an ultrasonic cleaner, and the cut PDMS into a plasma cleaner
162 for cleaning and bonding. After bonding, a complete microfluidic droplet generation chip is

163 obtained.

164 **2.6 ddPCR method**

165 According to the optimized reaction protocol and primers and probe concentrations from
166 qPCR, ddPCR experiments are conducted. The PCR reaction mixture serves as the aqueous
167 phase, and fluorinated oil (ThunderBio Innovation Limited, Hangzhou, Zhejiang, China) is
168 used as the oil phase. The experiment employs a droplet generation method based on negative
169 pressure formed by a vacuum pump, with the PCR reaction system serving as the aqueous
170 phase and the droplet generation oil as the oil phase. Driven by the negative pressure, the oil
171 and aqueous phases enter the cross-shaped channel of the droplet generation chip, where the
172 aqueous phase forms highly monodisperse droplets under the shear force of the oil phase.
173 Droplets are generated and collected in PCR tubes, followed by amplification. After spreading
174 the droplets using a homemade droplet spreading device, fluorescence images of the droplets
175 are acquired using the Olympus IX83 inverted fluorescence microscope (Olympus, Japan).
176 Droplet counting and size identification are performed using Cellpose [28] and ImageJ.
177 Cellpose is utilized for droplet recognition and segmentation, followed by quantification
178 using ImageJ. We fabricate the droplet spreading device through the following process: First,
179 we tightly adhere a 50 μm -thick PDMS film (Shenzhen, China) to the center of a disposable
180 petri dish. Subsequently, we mix epoxy resin AB glue at a 4:1 weight ratio, pour it into the
181 petri dish, and let it cure overnight at room temperature on a level surface. After the mold
182 fully cures, we peel it from the petri dish with the PDMS film-imprinted groove facing
183 upward. Next, we slowly pour the prepared PDMS solution (following Method 2.5) onto the
184 mold surface and cover it with a glass slide, taking care to avoid bubble formation during this
185 step. We then place the entire assembly in an 80°C oven for overnight curing. Finally, we
186 separate the glass slide with the cured PDMS—which serves as the upper cover of the device
187 —from the mold and assemble it with a glass counting chamber (Wuxi, China) that functions
188 as the base component.

$$C = \frac{P}{R} \times \frac{N}{V \times n}$$

189 where C is the logarithm of the bacterial concentration (CFU/mL), P is the number of positive
190 reaction units, R is the total number of reactions units, N is the total number of droplets
191 generated by the system, V is the volume of bacterial solution added to the system (mL), n is
192 concentration factor of the bacterial solution.

193 **2.7 Anti-interference evaluation**

194 In this study, two CC87 *L. monocytogenes* (MRL 300131 and MRL 300112) isolated from

195 food and clinical samples in our laboratory are selected as target detection strains, while the
196 reference strain *L. monocytogenes* EGD-e and the non-pathogenic *L. innocua* ATCC 33090
197 are used as interference strains to evaluate the anti-interference performance of the ddPCR
198 method. All strains are cultured in TSA-YE to the stationary phase as described in Section 2.1,
199 and the bacterial suspension concentration is adjusted to approximately 10^8 CFU/mL.
200 Subsequently, the CC87 target strains are mixed with each interference strain at ratios of 1:0,
201 1:1, and 0:1, respectively, to systematically evaluate the detection specificity and
202 anti-interference capability of ddPCR under mixed bacterial conditions.

203 **2.8 PMA-ddPCR method**

204 After treatment under the PMA processing conditions optimized in Section 2.4, detection is
205 performed using the ddPCR method described in Section 2.6. To verify the accuracy of the
206 PMA-ddPCR method in detecting viable bacteria, a mixed bacterial suspension of dead and
207 viable bacteria with a concentration of approximately 10^8 CFU/mL is prepared according to
208 the method described in Section 2.1. The mixed bacterial suspension is qualitatively verified
209 by staining with the BacLight™ Live/Dead Bacterial Viability Kit (Servicebio, Wuhan, China)
210 which contains two dyes, SYTO9 and propidium iodide (PI). Fluorescence images are
211 acquired using the Olympus IX83 inverted fluorescence microscope (Olympus, Japan), and
212 the images are processed using ImageJ software. Additionally, mixed samples of dead and
213 viable bacteria with different proportions of viable bacteria (100%, 50%, 25%, and 0%) are
214 prepared and subjected to comparative detection using both the plate counting method and the
215 PMA-ddPCR method to further validate the quantitative performance of this method under
216 conditions with varying proportions of viable bacteria.

217 **2.9 Data acquisition and analysis**

218 Data acquisition and analysis of fluorescence images are performed on MATLAB and
219 OriginPro 2021. All experiments are repeated three times. Data are presented as mean \pm
220 standard deviation (SD). Significance analysis (ANOVA) is conducted using GraphPad Prism
221 8.0.2 software, with a significance level of $p < 0.05$. Data processing and analysis are carried
222 out using OriginPro 2021.

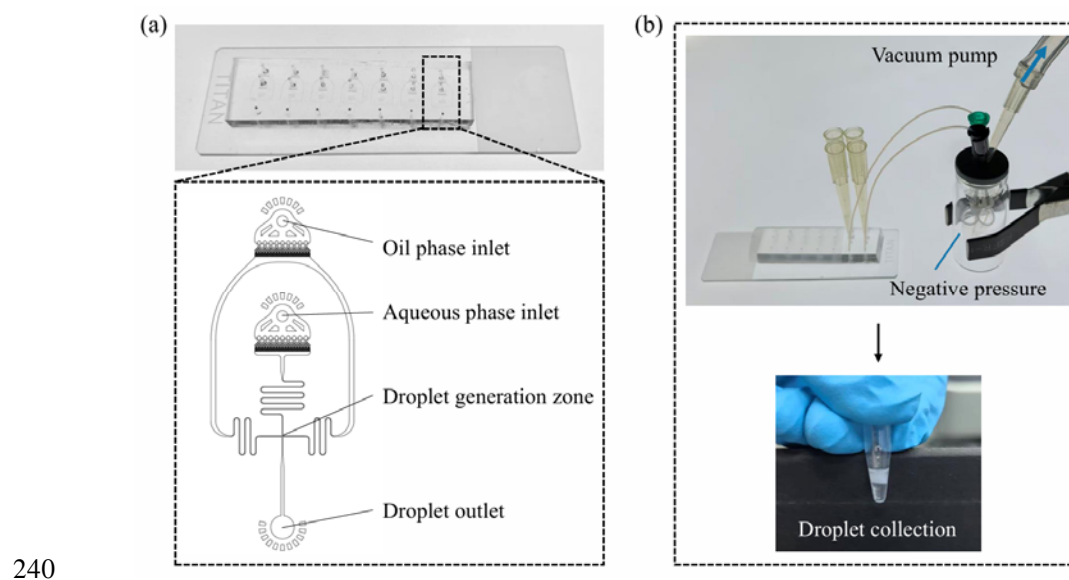
223

224 **3. Results**

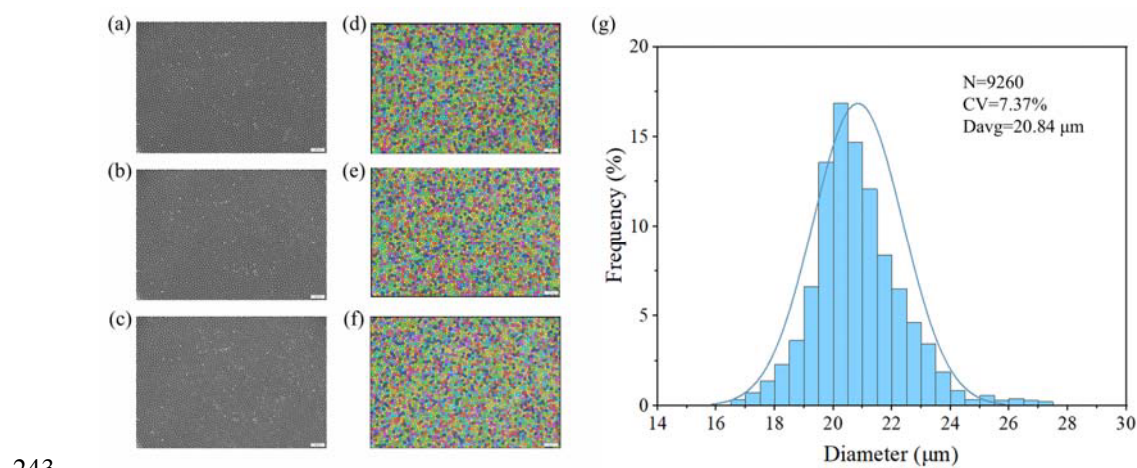
225 **3.1 Rapid generation and identification of uniform droplets**

226 We adopt a flow-focusing dropmaker design [29] to rapidly generate uniform droplets. In
227 brief, the design consists of an oil phase inlet, an aqueous phase inlet, a droplet generation
228 nozzle, and a droplet outlet. The complete design and image of the chip are shown in Fig. 2a.
229 We employ the suction droplet technique, driving the liquid flow by applying a vacuum at the

230 outlet, thereby enabling simple and rapid droplet generation. We achieve a generation rate of
231 approximately 2000 droplets per second per device. Notably, this straightforward suction
232 droplet scheme supports parallel droplet generation (Fig. 2b.), further enhancing the
233 efficiency of droplet production. The generated droplets are uniform in size and can be
234 quickly analyzed, with the entire detection process completed in approximately 3 hours. We
235 employ the Cellpose image processing technique, which accurately identifies droplets in
236 bright-field images (Fig. 3a-f.). We analyze the sizes of a total of 9260 droplets in three
237 independent experiments. The average diameter of these droplets is 20.84 μm , with a
238 coefficient of variation (CV) of 7.37% (Fig. 3g.), demonstrating a high degree of size
239 uniformity.



241 Fig. 2. (a) Physical diagram and schematic diagram of the droplet generation chip structure;
242 (b) Droplet generation device.

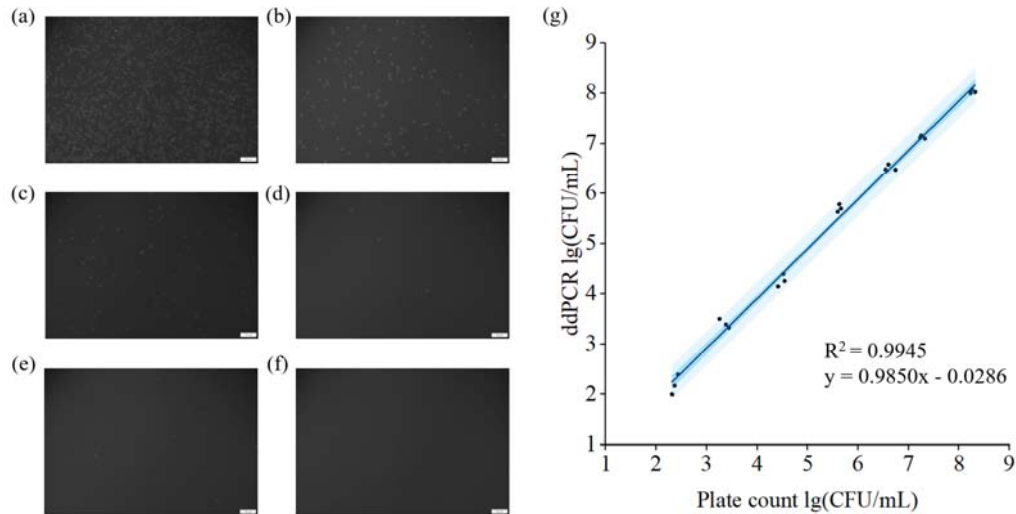


244 Fig. 3. (a) - (c) Bright-field images of monodisperse droplets. (d) - (f) Fluorescence images of
245 the same droplets after amplification, with false colors assigned by Cellpose image processing
246 software to indicate successful identification. (g) Droplet diameter distribution, showing high
247 uniformity. The average diameter is 20.84 μm with a coefficient of variation (CV) of 7.37%.

248 **3.2 Developing a rapid ddPCR quantification method**

249 We designed primers and probe (Table S1) for the successfully screened CC87-specific
250 sequences, and their high specificity was validated through Blast and qPCR experiments (Fig.
251 S2). The annealing temperature and primers/probe concentrations are optimized via qPCR,
252 and the optimized parameters are applied to ddPCR quantitative analysis. The results show
253 that the Ct value is the lowest and the fluorescence intensity Rn is the highest at an annealing
254 temperature of 50°C (Fig. S3), thus 50°C is determined as the optimal annealing temperature.
255 At a primers/probe concentration of 100/50 nM, the Ct value is the lowest, and there is no
256 significant difference in Ct values among the three groups of 100/50, 200/50, and 150/50 nM
257 ($p > 0.05$); while the Rn value reaches its highest at 300/50 nM, and there is no significant
258 difference in Rn values among the four groups of 300/50, 200/50, 300/100, and 250/50 nM
259 (Fig. S4). Considering both Ct values and Rn performance, the optimal primers/probe
260 concentration is ultimately selected as 200/50 nM. This condition ensures amplification
261 efficiency while significantly enhancing the differentiation between positive and negative
262 droplets, and also takes into account the economy and stability of the reaction.

263 With optimized reaction mixture, the ddPCR system accurately quantify bacteria over a wide
264 concentration range. We test the PCR system with a colony count range of approximately 10^2
265 to 10^8 CFU/mL as the aqueous phase. After droplet generation and amplification via a
266 microfluidic chip, the proportion of positive droplets is calculated through fluorescence
267 imaging analysis to determine the bacterial concentration. The ddPCR detection results
268 exhibit a high degree of consistency with the traditional plate counting method ($R^2 = 0.9945$,
269 Fig. 4. and Table S2), indicating that this method possesses excellent linear quantitative
270 capabilities, with a lower limit of quantification (LoQ) reaching 3.3×10^2 CFU/mL.

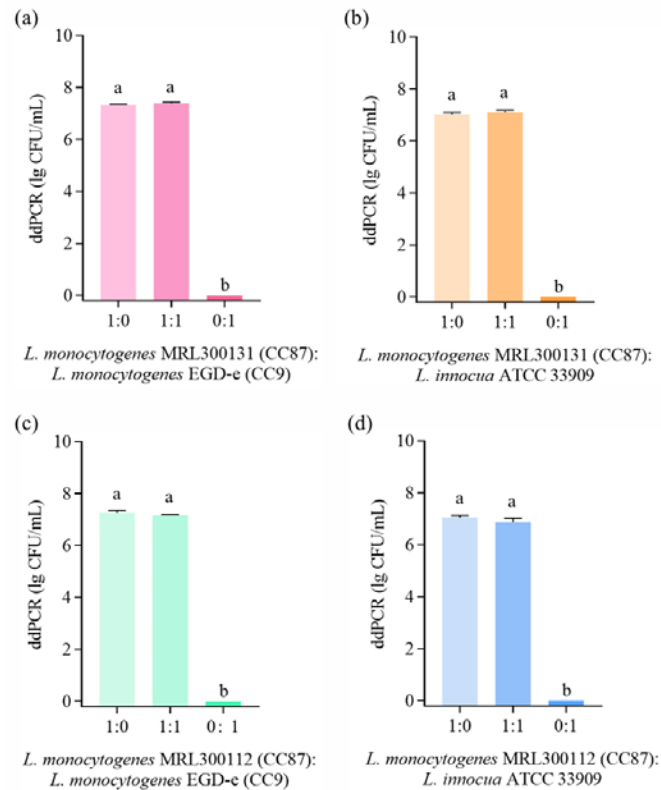


271

272 Fig. 4. Quantitative detection of CC87 *L. monocytogenes* using ddPCR method. Successfully
273 captured fluorescence field droplet images (a)-(f) under an inverted fluorescence microscope,
274 with corresponding bacterial solution concentrations of (a) 10^8 CFU/mL, (b) 10^7 CFU/mL, (c)
275 10^6 CFU/mL, (d) - (e) 10^5 CFU/mL, and (f) negative control with ddH₂O replacing the
276 bacterial solution; (g) Correlation between bacterial concentrations determined by the ddPCR
277 method and the plate counting method. The results show a high degree of consistency ($R^2 =$
278 0.9945), indicating the accuracy of the ddPCR assay.

279 3.3 Specific Detection and Quantification of the CC87 *L. monocytogenes* by ddPCR

280 In the context of complex mixed microbial communities, the ddPCR method established in
281 this study is capable of accurately identifying and quantifying CC types via primer specificity.
282 By mixing the CC87 strains (MRL 300131, MRL 300112) with competitive non-target strains
283 (*L. monocytogenes* EGD-e, *L. innocua* ATCC 33090) in different ratios, the anti-interference
284 performance of ddPCR was evaluated. The results show that even under mixed bacterial
285 conditions, the detection specificity of this method for the CC87 strains shows no significant
286 difference compared to pure culture ($p > 0.05$), confirming its excellent specificity and
287 anti-interference capability (Fig. 5.). This reproducible result confirms the anti-interference
288 capability and specificity of the detection system, providing a reliable technical tool for
289 addressing the monitoring challenges of specific subtypes in complex samples.



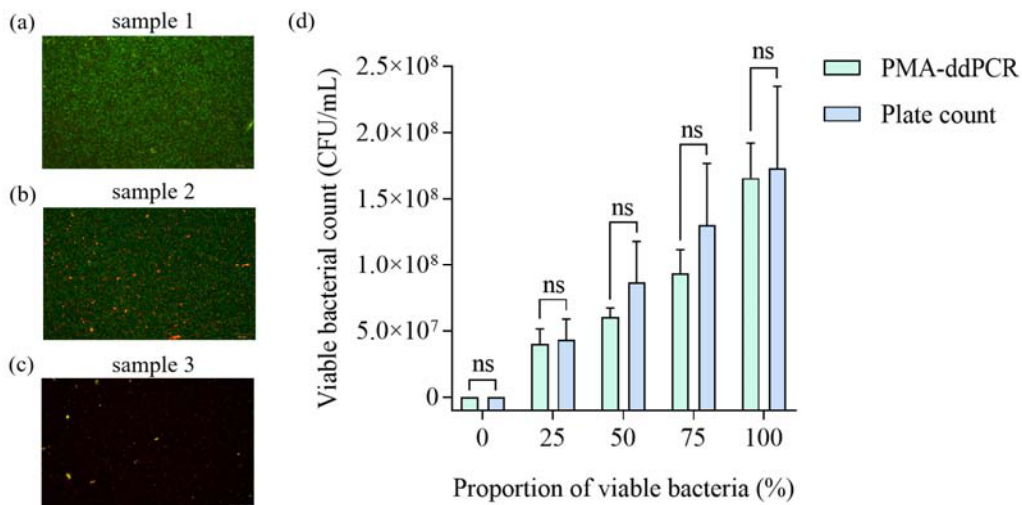
290

291 Fig. 5. Precise quantification of CC87 *L. monocytogenes* by ddPCR. *L. monocytogenes*
292 MRL300131 mixed with (a) *L. monocytogenes* EGD-e and (b) *L. innocua* ATCC 33909; *L.*
293 *monocytogenes* MRL300112 mixed with (c) *L. monocytogenes* EGD-e and (d) *L. innocua*
294 ATCC 33909. Same lowercase letters on the bars represent no significant differences, while
295 different letters represent significant differences among treatments ($p > 0.05$ was
296 non-significant).

297 3.4 Accurate differentiation and quantification of viable CC87 *L. monocytogenes* using 298 the PMA-ddPCR method

299 Because dead bacteria cause false positive results in ddPCR, this study integrates PMA
300 staining in the overall protocol to effectively remove dead bacteria signal and specifically
301 quantifies viable bacteria. We perform systematic optimization of PMA treatment conditions
302 and find that as the PMA concentration (20 ~ 80 μ M) increases, the Ct value of dead bacteria
303 significantly increases, while the amplification of viable bacteria remains unaffected ($p > 0.05$;
304 Fig. S5a), indicating that PMA selectively binds to dead bacterial DNA and inhibits its
305 amplification, thus determining 20 μ M as the optimal PMA treatment concentration.
306 Optimization experiments for dark incubation time show that when the dark incubation time
307 is ≥ 2 min, there is no significant difference in Ct values between viable and dead bacteria ($p >$
308 0.05; Fig. S5b), hence 2 min is selected as the optimal dark incubation time. The analysis of
309 the impact of different illumination durations on the amplification efficiency of viable and

310 dead bacteria reveals that within the range of 0 to 30 minutes, the amplification of viable
311 bacteria is unaffected; in contrast, the Ct value of dead bacteria significantly increases as the
312 illumination time increases from 0-15 minutes (Fig. S5c). Between 15 and 30 minutes, the Ct
313 value of dead bacteria shows no significant change ($p > 0.05$), and the amplification of viable
314 bacteria remains stable ($p > 0.05$). To maximize the elimination of interference from dead
315 bacteria amplification and to minimize the processing time, 15 minutes is ultimately
316 determined as the optimal illumination duration. The dCt values of viable bacteria are
317 generally close to 0 ± 1 , indicating that PMA does not affect the DNA amplification of viable
318 bacteria; whereas the dCt values of dead bacteria are greater than 8, equivalent to a removal
319 rate of approximately 99.6% of dead bacterial DNA. Additionally, we find that using different
320 resuspension/washing solutions in PMA treatment affects its efficacy. Among the three
321 resuspension/washing solutions, only PBS meets the requirements (Fig. S5d), maximizing the
322 inhibition of dead bacterial amplification without affecting the amplification of viable bacteria.
323 The BacLight™ Viability Kit is used for qualitative validation of the mixed bacterial
324 suspension (Fig. 6a-c.). Fluorescence microscopy analysis shows green fluorescence for
325 viable bacteria and red fluorescence for dead bacteria, providing a visual representation of the
326 composition of viable and dead bacteria in the sample. It is noteworthy that in mixed bacterial
327 suspension samples with different ratios, there is no significant difference in the quantitative
328 detection results of viable bacteria between the PMA-ddPCR method and the plate counting
329 method ($p > 0.05$; Fig. 6d. and Table S3). This result indicates that the PMA-ddPCR method
330 can accurately distinguish and quantify viable bacteria, effectively excluding the interference
331 of dead bacterial DNA, and achieving specific quantitative detection of viable CC87 *L.*
332 *monocytogenes*.



333

334 Fig. 6. Evaluation and detection of CC87 *L. monocytogenes* bacterial suspension. (a)-(c)
335 Fluorescence images of three distinct samples after staining with the SYTO9/PI Live-Dead

336 viability kit. Viable bacteria fluoresce green, and dead bacteria fluoresce red. The samples are
337 prepared as follows: Sample 1: A 1:10 dilution of a stationary-phase culture in PBS (~10⁸
338 CFU/mL). Sample 3: Heat-inactivated Sample 1. Sample 2: A 1:1 (v/v) mixture of Sample 1
339 and Sample 3. (d) Quantification of viable bacteria in mixed suspensions with varying
340 proportions of viable and dead cells, as determined by the PMA-ddPCR and plate counting
341 methods.

342

343 **4. Conclusion**

344 In summary, we present a PCR method based on droplet microfluidics for sensitive and rapid
345 detection of viable CC87 *L. monocytogenes* without nucleic acid extraction. The introduction
346 of the PMA treatment procedure effectively eliminates the interference of dead bacteria. The
347 droplet-based method has a LoQ for CC87 *L. monocytogenes* of 3.3×10^2 CFU/mL within 3h.
348 The method proposed in this study for the CC87 strains is an accurate and reliable
349 quantitative technique for monitoring the CC87 strains under mixed bacterial conditions, and
350 it can serve as a powerful tool for food safety assessment.

351

352 **Acknowledgments**

353 This work was supported by Qinghai Provincial Department of Science and Technology Key
354 Research and Development and Transformation Program (Grant No. 2025-QY-208), grants
355 from the National Key Research and Development Program of China (No.2023YFA0915200,
356 2023YFA0915204) and the National Natural Science Foundation of China (32102095). This
357 study was also supported by the equipment research and development projects of the Chinese
358 Academy of Sciences (PTYQ2024YZ0010), the equipment research and development
359 projects of the Chinese Academy of Sciences (PTYQ2024BJ0007), and the Science and
360 Technology Commission of Shanghai Municipality Project (XTCX-KJ-2024-038).

361

362 **References**

- 363 [1] N. Li, W. Zhang, G. Xing, Z. Wu, X. Wang, L. Lin, Chinese Chemical Letters (2025)
364 111704.
- 365 [2] J.A. Donaghy, M.D. Danyluk, T. Ross, B. Krishna, J. Farber, Front Microbiol 12 (2021)
366 668196.
- 367 [3] L. Chen, J. Wang, R. Zhang, H. Zhang, X. Qi, Y. He, J. Chen, Foods 11 (2022) 2382.
- 368 [4] Z. Li, Y. Wang, Z. Gao, S. Sekine, Q. You, S. Zhuang, D. Zhang, S. Feng, Y. Yamaguchi,
369 Analytica Chimica Acta 1251 (2023) 340995.

- 370 [5] E. Zhang, J. Cao, J. Cheng, G. Cai, S. Jiang, W. Xie, C. Jia, J. Zhao, S. Feng, Chinese
371 Chemical Letters (2025) 111109.
- 372 [6] World Health Organization. Food safety, 2024.
373 <https://www.who.int/news-room/fact-sheets/detail/food-safety> (Accessed 24 Nov 2025).
- 374 [7] H.B. Lee, K.H. Kim, G.A. Kang, K.-G. Lee, S.-S. Kang, Foods 11 (2022) 2948.
- 375 [8] X. Lu, H. Yang, Y. Wang, Y. Xie, IDR 16 (2023) 2793–2803.
- 376 [9] P.K. Roy, M.G. Song, S.Y. Park, Antioxidants 11 (2022) 1733.
- 377 [10] European Food Safety Authority, 2024. Story map on *Listeria monocytogenes*, available
378 online: <https://storymaps.arcgis.com/stories/629e6627e6c64111bfd5b9257473c74a> (Accessed
379 24 Nov 2025).
- 380 [11] S. Bolten, A.S. Harrand, J. Skeens, M. Wiedmann, Applied and Environmental
381 Microbiology 88 (2022) e00486-22.
- 382 [12] Z. Fan, J. Xie, Y. Li, H. Wang, Int J Infect Dis 81 (2019) 17–24.
- 383 [13] Y. Cheng, Q. Dong, Y. Liu, H. Liu, H. Zhang, X. Wang, Food Quality and Safety 6 (2022)
384 1–10.
- 385 [14] J. Liu, L. Yang, B.V. Kjellerup, Z. Xu, Trends in Microbiology 31 (2023) 1013–1023.
- 386 [15] C. Song, Y. Liu, R. Ding, H. Zhang, S. Feng, Current Opinion in Food Science 61 (2025)
387 101254.
- 388 [16] C. Lin, X. Li, T. Wu, J. Xu, Z. Gong, T. Chen, B. Li, Y. Li, J. Guo, Y. Zhang, BMEMat 1
389 (2023) e12007.
- 390 [17] L. Cao, L. Zeng, Y. Wang, J. Cao, Z. Han, Y. Chen, Y. Wang, G. Zhong, S. Qiao,
391 Microorganisms 12 (2024) 201.
- 392 [18] L. Hogekamp, S.H. Hogekamp, M.R. Stahl, PLOS ONE 15 (2020) e0232869.
- 393 [19] A.M. Nasrabadi, S. An, S.-B. Kwon, J. Hwang, Journal of Aerosol Science 115 (2018)
394 181–189.
- 395 [20] M.A. Nisar, K.E. Ross, M.H. Brown, R. Bentham, G. Best, H. Whiley, Frontiers in
396 Microbiology 14 (2023).
- 397 [21] Q. Yin, M. Nie, Z. Diwu, Y. Zhang, L. Wang, D. Yin, L. Li, Anal. Methods 12 (2020)
398 3933–3943.
- 399 [22] W. Xu, D. Shi, K. Chen, J. Palmer, D.G. Popovich, Journal of Microbiological Methods
400 214 (2023) 106830.
- 401 [23] X. Yang, Y. Zhong, D. Wang, Z. Lu, Anal. Methods 13 (2021) 5211–5215.
- 402 [24] J. Lee, C. Park, Y. Kim, S. Park, BioChip J 11 (2017) 287–293.
- 403 [25] W. Li, L. Bai, P. Fu, H. Han, J. Liu, Y. Guo, Foodborne Pathogens and Disease 15 (2018)

404 459–466.

405 [26] H. Zhang, W. Chen, J. Wang, B. Xu, H. Liu, Q. Dong, X. Zhang, *Front. Microbiol.* 11
406 (2020).

407 [27] M. Chen, J. Cheng, J. Zhang, Y. Chen, H. Zeng, L. Xue, T. Lei, R. Pang, S. Wu, H. Wu, S.
408 Zhang, X. Wei, Y. Zhang, Y. Ding, Q. Wu, *Front. Microbiol.* 10 (2019).

409 [28] M. Pachitariu, M. Rariden, C. Stringer. *bioRxiv.* (2025) 10.1101/2025.04.28.651001.

410 [29] S.L. Anna, N. Bontoux, H.A. Appl. Phys. Lett. 82 (2003) 364–366.

411

412 **Supplementary information**

413 Supplementary information associate with this article can be found.

414